ARTICLE
Journal of Cellular Biochemistry 116:2970–2979 (2015)

Journal of Cellular Biochemistry

The influence of MicroRNA-150 in Osteoblast Matrix Mineralization

Chun-Ling Dong,[1] Hao-Zhi Liu,[2] Zhen-Chun Zhang,[3] Huan-Li Zhao,[4] Hui Zhao,[3]* Yan Huang,[1] Jian-Hua Yao,[1] and Tian-Sheng Sun[1]

[1]*Department of Nursing, Linyi People's Hospital, Linyi 276003, P.R. China*
[2]*Department of Pharmacology, Linyi Health School, Linyi 276000, P.R. China*
[3]*Department of Rheumatism Immunity, Linyi People's Hospital, Linyi 276003, P.R. China*
[4]*Department of Orthopedics, Linyi People's Hospital, Linyi 276003, P.R. China*

ABSTRACT

This study investigated the influence of miR-150 expression on osteoblast matrix mineralization and its mechanisms. The mouse osteoblast cell line MC3T3-E1 was used as an in vitro model of bone formation. On the fifth day of mineralization, transfection experiments using agomiR-150, agomiR-NC, antagomiR-150 antagomiR-NC, and mock groups were set up to test the effects of miR-150 in MC3T3-E1 model. The mRNA and protein levels of OC, ALP, type I collagen, and OPN were measured by qRT-PCR and ELISA. Matrix mineralization was detected by alizarin red S (ARS) staining and flow cytometry was employed to quantify apoptosis in each group. RT-PCR and Western blot were applied to detect the expression of target gene *MMP14*. Our results demonstrated that the endogenous expression levels of miR-150, OC, ALP, type I collagen, and OPN in MC3T3-E1 cells increased steadily. Exogenous expressions of agomiR-150 and antagomiR-150 can significantly up-/down-regulate, respectively, the expression level of miR-150 in MC3T3-E1 cells. Compared with the mock group, higher expression levels of OC, ALP, type I collagen, and OPN mRNA were observed in the agomiR-150 group, while lower mRNA expression levels of OC, ALP, type I collagen, and OPN were found in the antagomiR-150 group. Based on these results, potential miR-150 targeted genes are discussed. Our results showed that miR-150 supports the osteoblastic phenotype related to osteoblast function and bone mineralization. Thus, miR-150 may have potential therapeutic applications in promoting bone formation in certain disease settings, such as in osteoporosis and in elderly patients. J. Cell. Biochem. 116: 2970–2979, 2015.

KEY WORDS: MINERALIZATION; OSTEOBLAST; MICRORNA-150; MIRNA AGOMIR; MIRNA ANTAGOMIR

Based on the force of impact, fractures are closed, with a limited dislocation angle, or open, with the displacement of extremities of the broken bone and accompanied by serious injury to the surrounding muscles, nerves, skin, and blood vessels [Henrotin, 2011]. Virtually millions of fractures occur every year in people all over the world caused by traumatic injury or other impact forces [Saito et al., 2014]. The prominent factors influencing bone fractures include age, gender, race, body constitution, lifestyle factors, and occupational hazards [Pressley et al., 2011; Looker, 2013; Johansson et al., 2014]. Fractures contribute considerably to the global health burden and in the United Kingdom the overall costs of managing fractures is close to £5.1 billion each year [Scholes et al., 2014; Siggeirsdottir et al., 2014]. Bone is one of the tissues that can heal without fibrous scar formation and bone healing occurs by tissue regeneration [Marsell and Einhorn, 2011]. In an attempt to recover full function and restore the anatomy, several treatment methods have been employed for treatment of fracture, including intramedullary nail fixation, plate and screw fixation, and surgical fixation [Drobetz et al., 2013; Stewart et al., 2013; Baldwin et al., 2014]. However, these methods are associated with highly variable outcomes, especially in elderly populations. In order to discover novel approaches to accelerate healing of fractures, it is essential to understand the underlying physiological processes and regulatory mechanisms.

The mechanisms of osteogenesis and osteoblast differentiation could be exploited for fracture treatment, particularly in osteoporotic patients and the elderly [Nakamura et al., 2015]. Substantial knowledge already exists in relation to bone growth and metabolism. Fibroblast growth factor 2 (FGF2) signaling plays a pivotal role in bone growth through activation of osteogenic master transcription

Conflict of interest: none.

*Correspondence to: Dr. Hui Zhao, Department of Rheumatism Immunity, Linyi People's Hospital, 27th Eastern Part of the Jiefang Road, Lanshan District, Linyi 276003, Shandong, P.R. China. E-mail: zhaohuizh555@163.com, s_tiansheng1025@yeah.net

Manuscript Received: 16 January 2015; Manuscript Accepted: 29 May 2015
Accepted manuscript online in Wiley Online Library (wileyonlinelibrary.com): 24 July 2015
DOI 10.1002/jcb.25245 • © 2015 Wiley Periodicals, Inc.

factor Runx2 [Yoon et al., 2014]. The stress hormones PGE2 (prostaglandin E2) and glucocorticoid influences osteoblast behavior through stimulating insulin-like growth factor I (IGF-I) expression [McCarthy et al., 2014]. In this respect, a broader regulation of osteoblast behavior is achieved by microRNAs (miRNAs) and they appear to tightly regulate osteoblast differentiation [Vimalraj et al., 2014]. The miRNAs are a large family of small non-coding (18–25 nucleotides) single-stranded RNAs that mediate gene suppression by binding to 3′ untranslated regions (3′ UTRs) of target mRNAs either promoting the degradation of target mRNAs or inhibiting their translation [Jia et al., 2013]. Further, miRNAs are key regulators of post-transcriptional gene expression and play pivotal roles in multiple cellular processes including transcription, translation, differentiation, apoptosis, autophagy, cell signaling, growth, and metabolism. Some miRNAs also collaborate with other microRNAs and RNA-binding proteins [Markou et al., 2013; Shenoy and Blelloch, 2014]. Osteoblast differentiation and osteogenesis are modulated by microRNAs which play an important role in transcriptional and post-transcriptional mechanisms [Chen et al., 2014]. Several miRNAs modulate osteogenic differentiation, for instance, miR-133, miR-135, and miR-125b inhibit the differentiation of osteoblastic differentiation while miR-26a and miR-29b positively modulate mouse osteoblast differentiation [Guo et al., 2011; Dong et al., 2012; Trompeter et al., 2013]. Modulation of miR-150 expression levels has a differential effect on natural killer (NK) and invariant NK T (iNKT) cell development [Bezman et al., 2011]. In addition, ectopic expression of miR-150 could promote tumorigenesis and proliferation of gastric cancer cells [Wu et al., 2010]. Moreover, the inhibition of miR-150 effectively arrests cell proliferation and promotes apoptosis, accompanied by increased p53 protein expression in lung cancer [Zhang et al., 2013]. In esophageal squamous cell carcinoma, the regulation by miR-150 could provide new direction for preventing metastasis and imply novel targeted therapeutic strategies [Yokobori et al., 2013]. To our knowledge, the involvement of miR-150 in osteoblast differentiation is not reported. Therefore, the present study investigated the physiological significance miR-150 expression in osteoblasts and its impact on osteoblasts function and mineralization.

MATERIALS AND METHODS

MOUSE CELL LINES

ROB-1, MC3T3-E1, MC3T3-E1 Subclone14, hFOBl.19, and SaOS-2 cell lines were grown in 1:1 mixture of F-12 and DMEM (F12/DMEM) containing 10% FBS (fetal bovine serum) and G418 (geneticin 300 g/ml) at 37°C in a humidified atmosphere of 5% CO_2. The culture medium was changed every 3–4 days. After cells reached 80% confluence, the culture medium was removed, cells were rinsed with PBS and detached using 0.25% pancreatic enzymes containing 0.02% EDTA for 3 min. The enzymes were inactivated by adding the complete culture medium and cells were counted and subcultured at a ratio of 1:4.

FLUORESCENCE QUANTITATIVE-PCR

Total RNA was isolated using Trizol (Invitrogen, Inc., Carlsbad, CA) according to the manufacturer's recommendations. The purity and concentration of RNA was determined by ultraviolet spectrophotometry. Agarose gel electrophoresis was employed to verify the integrity of RNA samples. After RNA was reverse transcribed to cDNA, miR-150 levels were quantified using Bulge-LoopTM miRNA qRT-PCR Primer Set kit (Ribobio, Guangzhou, China). The primers used for PCR were as follows: forward: 5′-CTCAACTGGTGTCGTGGAGTCGGCAATTCAGTTGAGCACTGGTA-3′; reverse: 5′-ACACTCCAGCTGGGTCTCCCAACCCTTGTA-3′. U6 was amplified as the internal control: forward: 5′-CTCGCTTCGGCAGCACA-3′; reverse: 5′-AACGCTTCACGAATTTGCGT-3′. The qRT-PCR conditions were as follows: 95°C for 12 s, 40°C for 3 min, and 62°C for 55 s for a total of 40 cycles. The Ct method was used for relative quantification of miR-150 expression using U6 as an internal control and $2^{-\Delta\Delta Ct}$ method was applied for data analysis. DNase/RNase-free H_20 was added in place of template as a negative control. The relative gene expressions in experimental group and control group was calculated by Folds $= 2^{-\triangle\triangle Ct}$: $\triangle\triangle Ct = (Ct_{(microRNA)} - Ct_{(U6)})_{experimental} - (Ct_{(microRNA)} - Ct_{(U6)})_{control}$. MC3T3-E1 cell line was considered as the control group and the other cell lines were experimental group. All experiments were repeated three times to calculate mean value.

CELL CULTURE

Cells were cultured in minimum essential medium (α-MEM) supplemented with 10% FBS, 100 U/ml penicillin, and 100 μg/ml streptomycin and grown in a humidified atmosphere at 37°C (5% CO_2 and 95% air) and the medium was replenished every 2–3 days until the cells were 80% confluent. The cultures were induced to differentiate by transferring the cells, after detachment, into culture medium supplemented with L-ascorbic acid and β-glycerol phosphate at final concentrations of 50 μg/ml and 10 mM, respectively.

CELL TRANSFECTION

MC3T3-E1 cells (2×10^4/ml) were seeded in 24-well plates and mineralization was induced when cells were 70% confluent (noted as day 0). The mineralization medium without antibiotic was replaced on fourth day after induction. On the fifth day, separate transfections were carried out with 5 μl agomiR-150, agomiR-negative control (agomiR-NC), antagomiR-150, and (antagomiR-negative control) antagomiR-NC in a volume of 250 μl α-MEM after a prior incubation of the transfection reagent mixed with the transfectants at room temperature for 5 min. The concentration of 400 nM was achieved during transfections. The transfected MC3T3-E1 cells were cultured at 37°C (5% CO_2 and 95% air). Five hours after the culturing, 250 μl of mineralization medium was added to continue the culture. Forty-eight hours after transfection, the expression levels of miR-150 and other osteoblast functional markers were detected. Mock transfection control was also set up to account for the effect of transfection conditions on miR-150 expression.

REAL-TIME QUANTITATIVE PCR (QRT-PCR)

Total RNA were isolated using Trizol reagent (Invitrogen, Inc.) and the purity and concentration of RNA were measured using ultraviolet spectrophotometry. In addition, RNAintegrity was checked by agarose gel electrophoresis. After reverse transcription and synthesis of cDNA template, Bulge-Loop™ miRNA qRT-PCR Primer Set (RiboBio Co, Guangzhou, China) was used to quantify

TABLE I. The Primer Sequences for Real-Time Quantitative Polymerase Chain Reaction for miR-150, U6, OC, β-Actin, ALP, Type I Collagen and OPN and GAPDH

Items	Primer	Sequence
miR-150	Forward	5′-CTCAACTGGTGTCGTGGAGTCGGCAATTCAGTTGAGCACTGGTA-3′
	Reverse	5′-ACACTCCAGCTGGGTCTCCCAACCCTTGTA-3′
U6	Forward	5′-CTCGCTTCGGCAGCACA-3′
	Reverse	5′-AACGCTTCACGAATTTGCGT-3′
OC	Forward	5′-AGGAGGGCAATAAGGTAGT-3′
	Reverse	5′-CATAGATGCGTTTGTAGGC-3′
β-actin	Forward	5′-CTGTCCCTGTATGCCTCT-3′
	Reverse	5′-TGATGTCACGCACGATTT-3′
ALP	Forward	5′- TGGCTCTGCCTTTATTCCCTAGT-3′
	Reverse	5′-AAATAAGGTGCTTTGGGAATTGT-3′
Type I collagen	Forward	5′-CTTGGTCTCGTCACAGATCA-3′
	Reverse	5′- CTTTTAACGGAGGATGTGCTATTTGGG-3′
OPN	Forward	5′- GCCATCACCCTGTCTCCTAA-3′
	Reverse	5′-GCTGTGGAGAAGACACACGA-3′
GAPDH	Forward	5′-CATCCCAGAGCTGAACG-3′
	Reverse	5′-CTGGTCCTCAGTGTAGCC-3′

OC, osteocalcin; ALP, alkaline phosphatase; OPN, osteopontin; GAPDH, glyceraldehyde-3-phosphate dehydrogenase.

miR-150 expression. The temperature profile of the reaction was 95°C for 3 min followed by 95°C for 12 s and 40 cycles of extension at 62°C for 55 s. The relative quantities for miR-150 were determined by the comparative Ct method ($2^{-\Delta\Delta Ct}$), where $\Delta Ct = (Ct_{miRNA} - Ct_{U6})$. The mRNA was detected using Maxima SYBR Green/ROX qPCR Master Mix (Fermentas, Canada). The relative quantities for OC were determined by the comparative Ct method ($2^{-\Delta\Delta Ct}$), where $\Delta Ct = (Ct_{miRNA} - Ct_{\beta\text{-actin}})$. The mRNAs of osteocalcin (OC), alkaline phosphatase (ALP), type I collagen, and osteopontin (OPN) were analyzed using Maxima SYBR Green/ROX ePCR Master Mix (Fermentas). The RT-PCR condition were: predenaturing at 95°C for 10 min, denaturing at 95°C for 10 s, annealing at 60°C for 30 s, and extension at 72°C for 30 s, for a total of 40 cycles. The relative quantities were determined by the comparative Ct method ($2^{-\Delta\Delta Ct}$) with β-actin as an internal control. The primer sequence of miR-150, OC, ALP, type I collagen and OPN, and internal controls are shown in Table I.

ENZYME-LINKED IMMUNOSORBENT ASSAY (ELISA)

After 48 h of transfection, the culture supernatants from MC3T3-E1 groups were collected and centrifuged at 1,000 rpm for 20 min. The cleared supernatant was used to measure the protein levels of OC, ALP, type I collagen, and OPN using double-antibody sandwich ELISA kit (WHO, Geneva). The micro-plate wells were pre-coated with respective antibodies and the OC/ALP/type I collagen/OPN standards (100 μl), for the standard curve, and diluted standards (100 μl) for blank control were added into each well. Subsequently, biotinylated antibodies for OC/ALP/type I collagen/OPN were added into wells. After three washes, horseradish peroxidase-conjugated streptavidin was added, followed by thorough washing of the wells to remove all unbound components. TMB substrate was added for chromogenic detection and optical density (OD) was measured at 490 nm using microplate reader.

MEASUREMENT OF MINERALIZATION USING ALIZARIN RED S (ARS) STAINING

On the 11th and 17th days after the induction of mineralization, MC3T3-E1 cells were similarly transfected for the second and third time. Cells were stained with calcium alizarin red staining kits (Genmed Scientifics, Inc., USA) on the 21st day after mineralization. ARS staining was quantified by UV spectrophotometer by measuring the absorbance (A) at 540 nm. The A value of pure cells without ARS staining after adjusting pH by adding chloride cetyltrimethylammonium solution was also measured. Results of Alizarin Red staining were expressed as ng/mg protein. Experiments were repeated five times, and average and standard deviation (SD) were calculated.

THE TARGET GENES OF MMU-MIR-150

In the current study, TargetScan, PicTar microRNA.org software were employed to identify possible mmu-miR-150 target genes. The 3′ UTR of *MMP14* gene was cloned into the multiple cloning sites of GV126-Luciferase (Promega Corporation). Site-directed mutagenesis was used to abolish mmu-miR-150 binding site on *MMP14* gene. Renilla luciferase expression vector, pRL-TK vector, was used as internal control (Takara, Shiga, Japan). NC and agomiR-150 with luciferase expression vector were transfected to HEK293 cells. The Dual-Luciferase Reporter kit (Promega) was used for detection of the luciferase activity according to manufacturer's protocol.

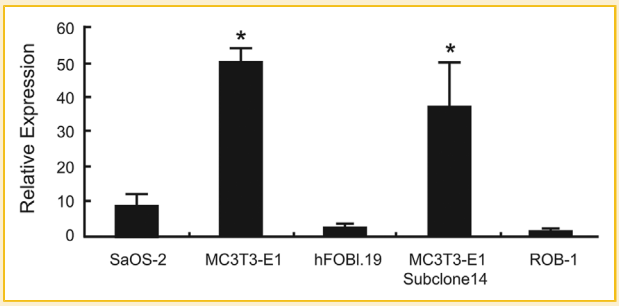

Fig. 1. The expression levels of miR-150 in ROB-1cell line, SaOS-2 cell line, MC3T3-E1 cell line, hFOBl.19 cell line, and MC3T3-E1 Subclone14 cell lines.

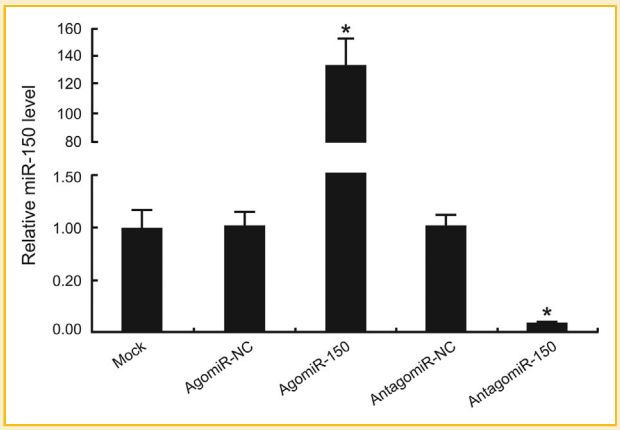

Fig. 2. After transfection for 48 h, the expression level of miR-150 in MC3T3-E1 cells in mock group, agomiR-NC group, agomiR-150 group, antagomiR-NC group, and antagomiR-150 group.

EXPRESSION OF MMP14 MRNA BY RT-PCR

RNA from MC3T3-E1 cells transfected with agomiR-150 and antagomiR-150 were extracted at 48 h to observe the MMP14 mRNA expression. Primers for MMP14 were as follows: forward: 5′-GCTGGCAATTTGGTGTGCTC-3′; reverse: 5′-TGGTTTGGGTATG-CACCTTTGG-3′. The amplified product size was 251bp. Primers were synthesized by GenScript Co., Ltd (Nanjing). Human GAPDH primers were used as control: forward: 5′-TCATTGACCTCAACTA-CATG-3′; reverse: 5′-GCAGTGATGGCTTGGACTGT-3′. The amplified product size was 439bp. MMP14 was quantified using the same method for OC detection.

EXPRESSION OF MMP14 BY WESTERN BLOT

After cell-lysis, the protein concentration of the lysate was determined using BCA (protein concentration determination) protein assay kit. An amount of 50 μg total protein per sample was run on 10% sodium dodecyl sulfate-polyacrylamide gel electrophoresis (SDS-PAGE) gel, followed by wet-transfer process using polyvinylidene fluoride (PVDF) membrane. Then the reaction was blocked with 50% skim milk powder at room temperature. Samples were added withMMP14 (1:1,000) and β-actin (1:5,000) first antibodies for overnight reaction in a shaking table at 4°C. After repeated washing, the samples were incubated for 1 h at room temperature with the addition of secondary antibody goat anti-rabbit (1:2,000) (Abcam, Inc., Cambridge, MA) conjugated with horseradish peroxidase (HRP). Blots were developed with the ECL Plus reagent (Amersham). Gray value was determined by gel imaging system

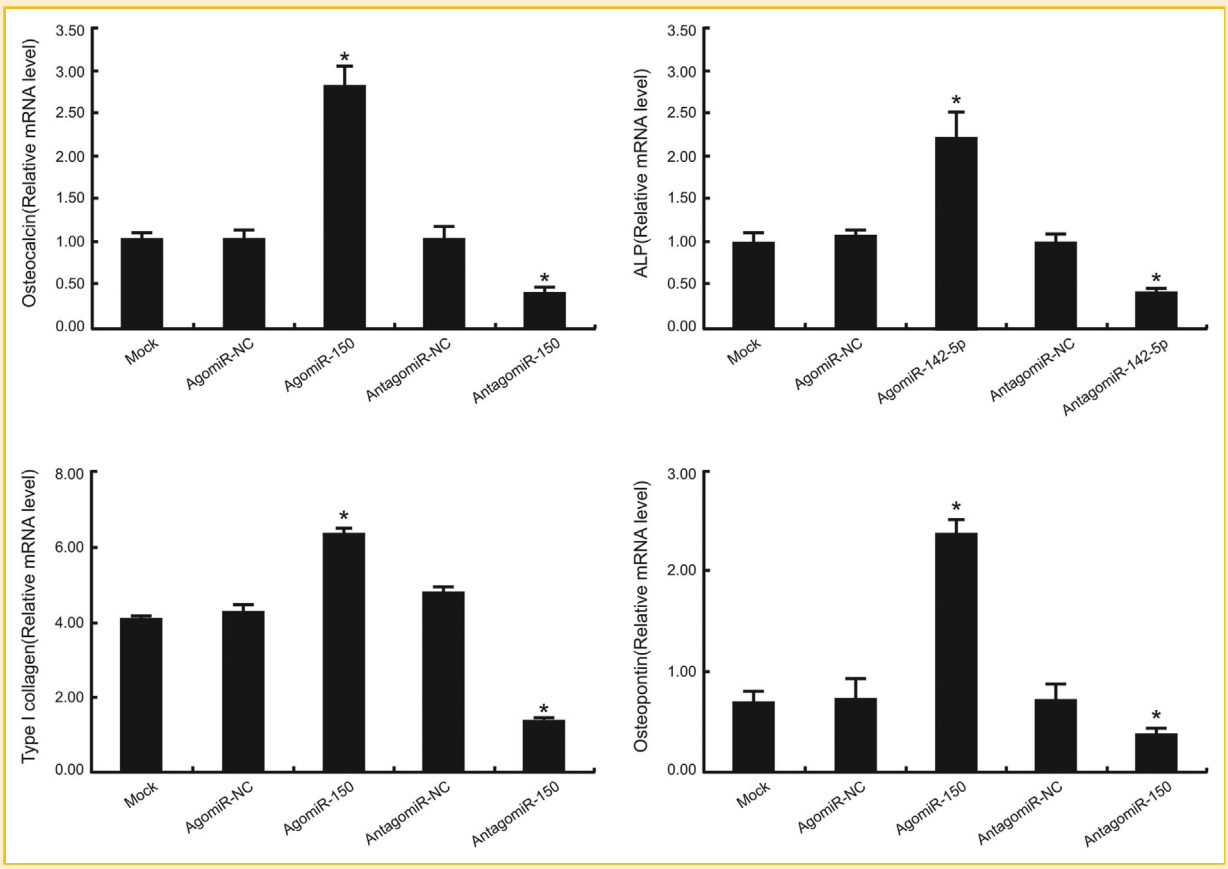

Fig. 3. After transfection for 48 h, the mRNA expression of OC, ALP, type I collagen, and OPN in MC3T3-E1 cell culture supernatant in mock group, agomiR-NC group, agomiR-150 group, antagomiR-NC group, and antagomiR-150 group by reverse transcription quantitative real-time polymerase chain reaction (RT-qPCR).

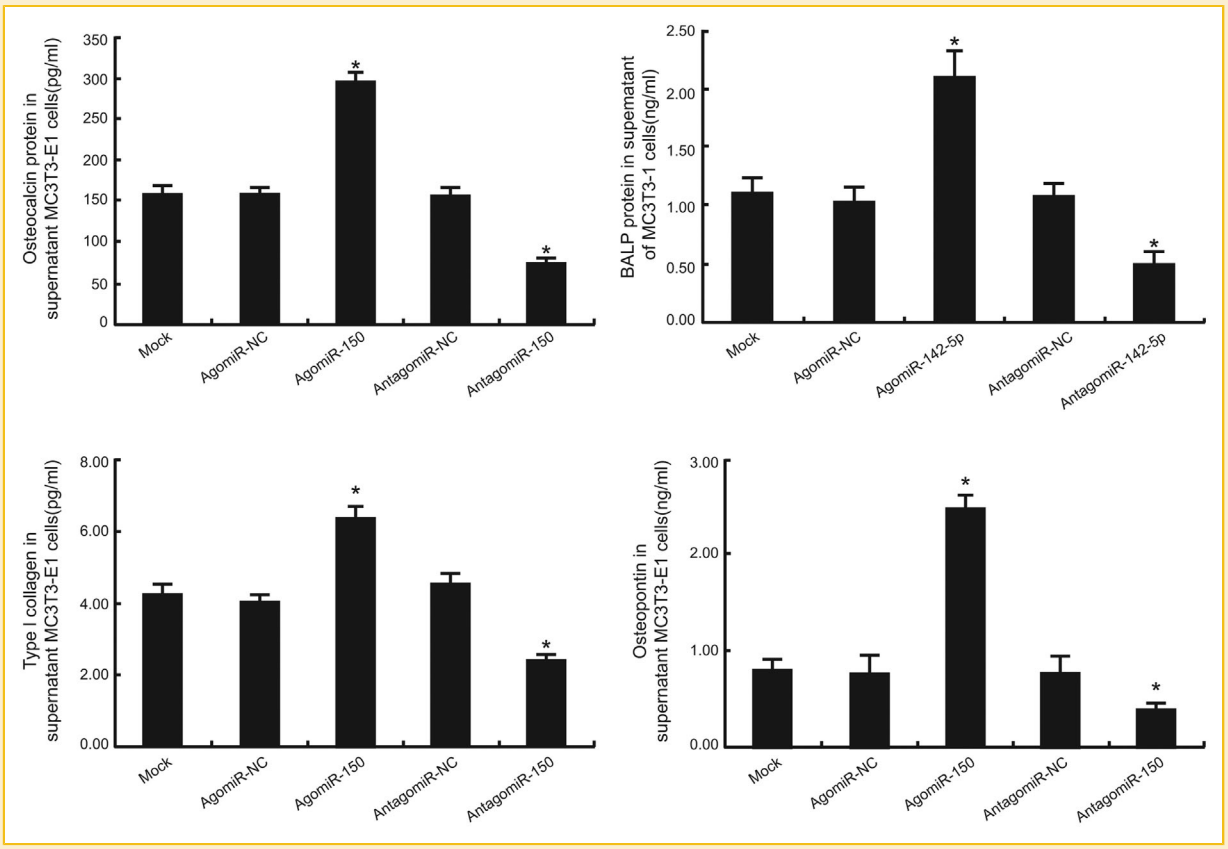

Fig. 4. After transfection for 48 h, the protein expression of OC, ALP, type I collagen, and OPN in MC3T3-E1 cell culture supernatant in mock group, agomiR-NC group, agomiR-150 group, antagomiR-NC group, and antagomiR-150 group by enzyme-linked immunosorbent assay (ELISA).

(Synegene Ltd., Cambridge, MA) and quantification was done using Gene Tools software (Synegene Ltd.).

APOPTOSIS BY FLOW CYTOMETER

After MC3T3-E1 cells were transfected with agomiR-150, agomiR-NC, antagomiR-150, antagomiR-NC, MMP14 inhibitor, and MMP14 inhibitor-NC, the cells in logarithmic growth phase were seeded in to 6-well plates at a cell density of 1×10^6/mL. The non-transfected cells were considered as Mock group. The samples were digested with 0.25% trypsin (without EDTA). Cell suspension (1.5 ml) was centrifuged at 1,000 rpm for 5 min. After removing the medium, the samples were washed with PBS twice and centrifuged for 5 min at 2,000 rpm. Subsequently, $1–5 \times 10^5$ cells were collected and 500 μl binding buffer of annexin VFITC (5.1 μl) and propidium iodide (5 gl) was added. After mixing, the samples were placed at room temperature in dark for 5–15 min. Flow cytometry was used to measure apoptosis within an hour.

STATISTICAL ANALYSIS

SPSS 18.0 software (SPSS Inc., Chicago, IL) was used for all statistical analyses. Continuous data were presented as mean ± SD. The differences between control and case group were compared using

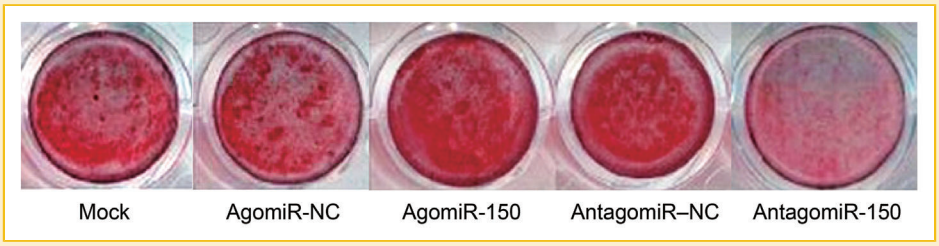

Fig. 5. The results of alizarin red S staining in mock group, agomiR-NC group, agomiR-150 group, antagomiR-NC group, and antagomiR-150 group at 21st day after induced mineralization of MC3T3-E1 cells.

t-test. Comparisons of means were performed using LSD (t) test. Categorical data were expressed as frequency or counts and χ^2 was used to compare the frequencies. Comparisons among groups were tested by homogeneity of variance test and one-way ANOVA analysis. All tests were two-sided with $P < 0.05$ considered statistically significant.

RESULTS

MIR-150 EXPRESSIONS IN CELL LINES

Fluorescence quantitative-PCR was employed to measure miR-150 expression levels in ROB-1, MC3T3-E1, MC3T3-E1 Subclone14, hFOBl.19, and SaOS-2 cell lines. ROB-1 cell line was selected as the control group with 1.000 ± 0.000. PCR results demonstrated that miR-150 in SaOS-2, MC3T3-E1, hFOBl.19, and MC3T3-E1 Subclone14 cell lines were 8.264 ± 3.154, 48.265 ± 6.481, 2.458 ± 1.026, 37.256 ± 5.148, respectively (Fig. 1). One-way ANOVA analysis showed statistically significant differences in miR-150 expression among the five cell lines ($P < 0.05$). MC3T3-E1 cell line showed the highest expression level, compared to hFOBl.19, SaOS-2, MC3T3-E1 Subclone14, and ROB-1 cell lines ($P < 0.05$). Therefore, MC3T3-E1 cell line was selected for further analysis.

EXPRESSION OF MIR-150 AFTER TRANSFECTION

No statistical difference in miR-150 expression level was detected among agomiR-NC group, antagomiR-NC, and the mock group ($P > 0.05$). The miR-150 expression level in agomiR-150 group increased markedly compared to agomiR-NC group ($P < 0.05$).

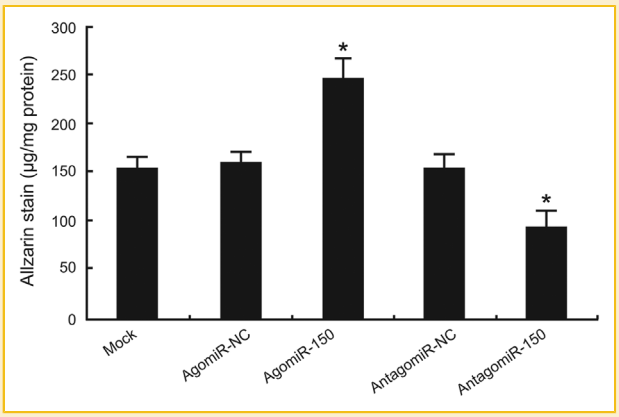

Fig. 6. Alizarin red S (ARS) staining for MC3T3-E1 cells in mock group, agomiR-NC group, agomiR-150 group, antagomiR-NC group, and antagomiR-150 group at 21st day after induced mineralization of MC3T3-E1 cells.

Conversely, miR-150 expression level in antagomiR-150 group was lower than antagomiR-NC group ($P > 0.05$) (Fig. 2).

UP-REGULATION OF OC EXPRESSION BY MIR-150

RT-PCR was used to detect the expression levels of OC, ALP, type I collagen, and OPN mRNA in MC3T3-E1 cells 48 h after transfection during osteoblastic-cell differentiation. The results demonstrated markedly higher expression levels of OC, ALP, type I collagen, and OPN mRNA inagomiR-150 group compared to agomiR-NC group. Consistent with this, lower mRNA levels of OC,

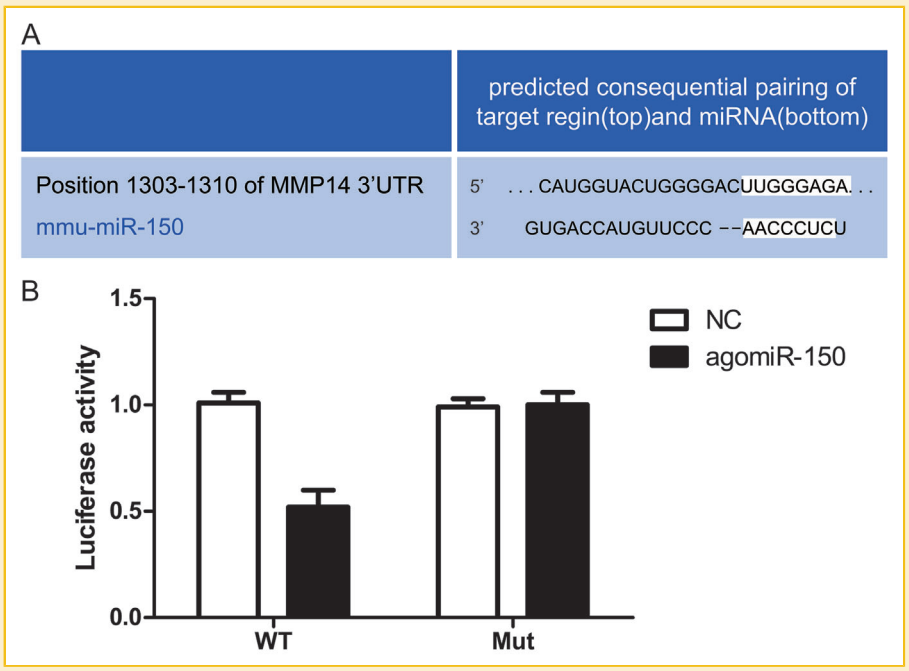

Fig. 7. miR-150 target MMP14 (A: TargetScan identified the binding site of miR-150 and MMP14 3′ UTR; B: miR-150 target MMP14 identified by dual-luciferase reporter assay).

ALP, type I collagen, and OPN were found in the antagomiR-150 group compared to antagomiR-NC group (both $P < 0.05$). ELISA results showed significantly higher OC , ALP, type I collagen, and OPN protein levels in agomiR-150 group compared to agomiR-NC group, and markedly lower OC, ALP, type I collagen, and OPN protein levels in antagomiR-150 group compared to antagomiR-NC group (both $P < 0.05$), which was consistent with our RT-PCR results (Figs. 3 and 4).

THE ROLE OF MIR-150 IN MATRIX MINERALIZATION OF MC3T3-E1 CELLS

A remarkable increase in ARS staining was observed in the agomiR-150 group compared to agomiR-NC group and a significant decrease was found in antagomiR-150 group compared to antagomiR-NC group at day 21 after induction of mineralization in MC3T3-E1 cells (both $P < 0.05$) (Figs. 5 and 6).

MIR-150 TARGET *MMP14*

TargetScan software found that miR-150 directly binds to MMP14 3′ UTR (Fig. 7A). Wild-type and mutant GV126-MMP14 3′ UTR were constructed. HEK293 cells were variously transfected with miR-150 mimics and *MMP14* constructs, and dual-luciferase reporter assay was used to observe gene expression. The results revealed that luciferase signal of *MMP14* wild-type diminished 50% compared with mock group and no significant change in luciferase signal was observed with *MMP14* mutant vector (Fig. 7B). Our results suggested that *MMP14* is a target gene of miR-150.

IDENTIFICATION OF MIR-150 TARGET GENE

MMP14 mRNA was detected by RT-qPCR and MMP14 protein level was visualized using western blots (Figs. 8 and 9). Our results demonstrated that agomiR-150 expression significantly down-regulated MMP14 protein levels compared with agomiR-NC ($P < 0.05$), whereas antagomiR-150 up-regulated MMP14 protein levels compare to antagomiR-NC, with statistical significance ($P < 0.05$). Our study also found that agomiR-150 and antagomiR-150 can up- or down-regulate, respectively, the MMP14 mRNA levels.

APOPTOSIS OF MC3T3-E1 CELL LINE

Apoptosis rates were measured in mock group, antagomiR-NC group, antagomiR-150 group, agomiR-150 group, agomiR-NC group, MMP14 inhibitor group, and MMP14 inhibitor-NC group and the apoptosis rates were 18.13, 11.90, 30.15, 4.10, 10.00, 3.80, and 9.00%, respectively. The apoptosis results revealed that MMP14 inhibitor group and agomiR-150 group had the lowest apoptosis rates compared to the other five groups (all $P < 0.05$) and no significant difference was found between the MMP14 inhibitor group and agomiR-150 group ($P > 0.05$). Moreover, antagomiR-150 group showed the highest apoptosis rate (all $P < 0.05$) (Fig. 10).

DISCUSSION

The present study investigated the effects of miR-150 on osteoblast differentiation to understand the physiological mechanisms

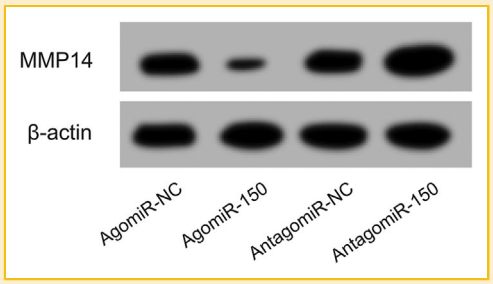

Fig. 8. After transfection for 48 h, MMP14 protein expression level in MC3T3-E1 cells in agomiR-NC group, agomiR-150 group, antagomiR-NC group, and antagomiR-150 group by Western hybridization.

involved in bone formation. In this study, we used MC3T3-E1 cells to induce osteoblast differentiation and the successful induction was confirmed by elevated expression levels of osteoblast markers OC, ALP, type I collagen, and OPN in agomiR-150 group compared to controls. Our data showed that exogenous addition of agomiR-150 or antagomiR-150 up- or down-regulated the levels of OC, ALP, type I collagen, and OPN in MC3T3-E1 cells compared to controls, suggesting that increased miR-150 levels increased osteoblast function and promoted bone mineralization for bone formation.

In the current study, TargetScan software was used to identify possible miR-150 target genes and we identified MMP14 as a novel miR-150 target. Bioinformatics-based analysis showed that miR-150 targets 3′ UTR of MMP14. A potential explanation for our results could be that miR-150 influences the expression of OC, ALP, type I collagen, and OPN by targeting MMP14 gene. Matrix metalloproteinases (MMPs) are important for angiogenesis, cell invasion, and metastases in malignant tumors [Akanuma et al., 2014]. MMP-

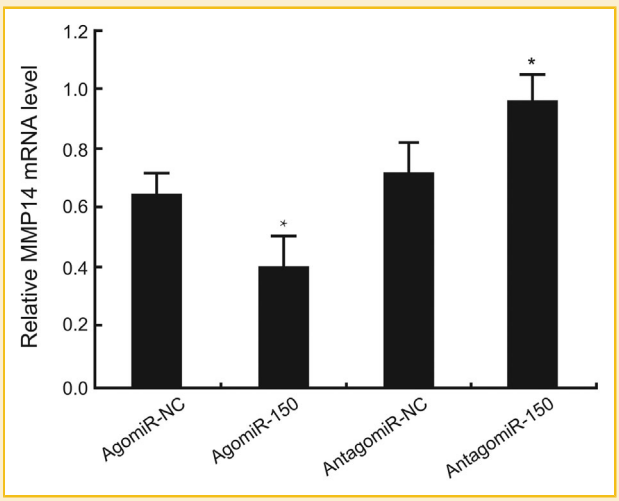

Fig. 9. After transfection for 48 h, MMP14 mRNA expression level in MC3T3-E1 cells in agomiR-NC group, agomiR-150 group, antagomiR-NC group, and antagomiR-150 group by reverse transcription quantitative real-time polymerase chain reaction (RT-qPCR).

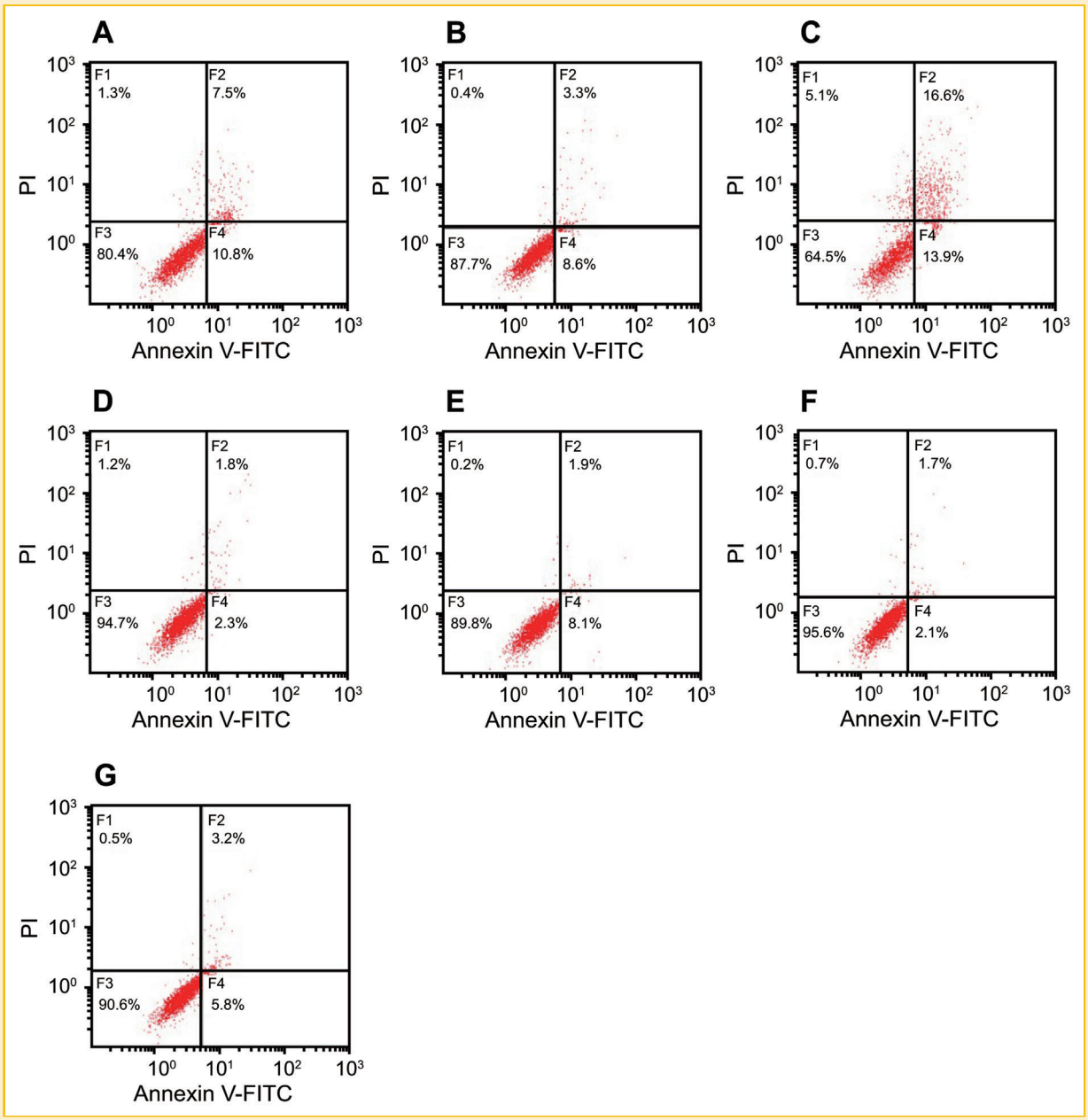

Fig. 10. The apoptosis of MC3T3-E1 cell line by flow cytometer (A: mock group; B: antagomiR-NC group; C: antagomiR-150 group; D: agomiR-150 group; E: agomiR-NC group; F: MMP14 inhibitor group; G: MMP14 inhibitor-NC group).

14, also referred to as MT1-MMP, is expressed on the cell surface and has broad substrate specificities [Nakai et al., 2013]. MMP14 plays an important role in cancer metastasis by degrading extracellular matrix (ECM) components and increasing the secretion of proMMP2 and proMMP9 through their complex formation (proMMP-2/TIMP-2 and proMMP-9/TIMP-1 complexes) [Egawa et al., 2006]. Importantly, MMP-14 exhibits potent collagenase activity and MMP-14 plays a dual role in collagen degradation through its collagenolytic activity and in the activation of proMMP-2 and proMMP-13 [Shiomi et al., 2010]. Akanuma et al. [2014] demonstrated that the knockdown of MMP14 inhibited the proliferation and invasion of esophageal squamous cell carcinoma cells, suggesting that MMP14expression is associated with poor prognosis in esophageal squamous cell carcinoma. Evidence also shows that elevated expression of MMP-2, MMP-7, and MMP14 is closely associated with differentiation, portal invasion, intrahepatic metastasis, and recurrence in hepatocellular carcinoma [Miyoshi et al., 2005]. Paiva et al. showed that MMP-14 transcript levels are down-regulated throughout osteoblast differentiation (Paivaa KB, Bendinia N, Silvaa LH, et al. Expression of membrane-type matrix metalloproteinases (MT-MMPS) during osteoblast differentiation [J]). Our results are consistent with these previous observations.

Our results revealed that transfection of agomiR-150 up-regulated both the mRNA and protein levels of OC, ALP, type I collagen, and OPN in MC3T3-E1 cells, promoting mineralized nodule formation and increasing the intensity of quantitative alizarin red used to detect mineralized nodule formation [Kato et al., 2013]. Apoptosis assay demonstrated that the inhibition of MMP14 and agonist miR-150 can significantly reduce apoptosis rate, while the inhibition of miR-150 led to increased apoptosis. Therefore, miR-150 indeed binds to MMP14 and decreases MMP14 expression, indicating a negative regulation of MMP14 by miR-150 relevant to osteoblast functions. Consistent with our results, Ni et al. reported that inhibition of miR-150 arrested cell proliferation and promoted apoptosis in lung cancers [Zhang et al., 2013].

In conclusion, our study revealed that miR-150 expression stimulated osteoblast function and promoted osteoblast mineralization for bone formation by negatively regulating MMP14. Therefore, mechanisms related to miR-150 may be considered as a potential novel therapeutic strategy to promote bone formation. However, further studies are required to confirm our results from in vivo observations.

ACKNOWLEDGEMENT

The authors wish to express their appreciation to reviewers for their critical comments.

REFERENCES

Akanuma N, Hoshino I, Akutsu Y, Murakami K, Isozaki Y, Maruyama T, Yusup G, Qin W, Toyozumi T, Takahashi M, Suito H, Hu X, Sekino N, Matsubara H. 2014. MicroRNA-133a regulates the mRNAs of two invadopodia-related proteins, FSCN1 and MMP14, in esophageal cancer. Br J Cancer 110:189–198.

Baldwin K, Morrison MJ, 3rd, Tomlinson LA, Ramirez R, Flynn JM. 2014. Both bone forearm fractures in children and adolescents, which fixation strategy is superior – plates or nails? A systematic review and meta-analysis of observational studies. J Orthop Trauma 28:e8–e14.

Bezman NA, Chakraborty T, Bender T, Lanier LL. 2011. MiR-150 regulates the development of NK and iNKT cells. J Exp Med 208:2717–2731.

Chen L, Holmstrom K, Qiu W, Ditzel N, Shi K, Hokland L, Kassem M. 2014. MicroRNA-34a inhibits osteoblast differentiation and in vivo bone formation of human stromal stem cells. Stem Cells 32:902–912.

Dong S, Yang B, Guo H, Kang F. 2012. MicroRNAs regulate osteogenesis and chondrogenesis. Biochem Biophys Res Commun 418:587–591.

Drobetz H, Weninger P, Grant C, Heal C, Muller R, Schuetz M, Pham M, Steck R. 2013. More is not necessarily better. A biomechanical study on distal screw numbers in volar locking distal radius plates. Injury 44:535–539.

Egawa N, Koshikawa N, Tomari T, Nabeshima K, Isobe T, Seiki M. 2006. Membrane type 1 matrix metalloproteinase (MT1-MMP/MMP-14) cleaves and releases a 22-kDa extracellular matrix metalloproteinase inducer (EMMPRIN) fragment from tumor cells. J Biol Chem 281:37576–37585.

Guo L, Zhao RC, Wu Y. 2011. The role of microRNAs in self-renewal and differentiation of mesenchymal stem cells. Exp Hematol 39:608–616.

Henrotin Y. 2011. Muscle: A source of progenitor cells for bone fracture healing. BMC Med 9:136.

Jia J, Tian Q, Ling S, Liu Y, Yang S, Shao Z. 2013. MiR-145 suppresses osteogenic differentiation by targeting Sp7. FEBS Lett 587:3027–3031.

Johansson H, Kanis JA, Oden A, McCloskey E, Chapurlat RD, Christiansen C, Cummings SR, Diez-Perez A, Eisman JA, Fujiwara S, Gluer CC, Goltzman D, Hans D, Khaw KT, Krieg MA, Kroger H, LaCroix AZ, Lau E, Leslie WD, Mellstrom D, Melton LJ, 3rd, O'Neill TW, Pasco JA, Prior JC, Reid DM, Rivadeneira F, van Staa T, Yoshimura N, Zillikens MC. 2014. A meta-analysis of the association of fracture risk and body mass index in women. J Bone Miner Res 29:223–233.

Kato H, Katayama N, Taguchi Y, Tominaga K, Umeda M, Tanaka A. 2013. A synthetic oligopeptide derived from enamel matrix derivative promotes the differentiation of human periodontal ligament stem cells into osteoblast-like cells with increased mineralization. J Periodontol 84:1476–1483.

Looker AC. 2013. Femur neck bone mineral density and fracture risk by age, sex, and race or Hispanic origin in older US adults from NHANES III. Arch Osteoporos 8:141.

Markou A, Sourvinou I, Vorkas PA, Yousef GM, Lianidou E. 2013. Clinical evaluation of microRNA expression profiling in non small cell lung cancer. Lung Cancer 81:388–396.

Marsell R, Einhorn TA. 2011. The biology of fracture healing. Injury 42:551–555.

McCarthy TL, Yun Z, Madri JA, Centrella M. 2014. Stratified control of IGF-I expression by hypoxia and stress hormones in osteoblasts. Gene 539:141–151.

Miyoshi A, Kitajima Y, Kido S, Shimonishi T, Matsuyama S, Kitahara K, Miyazaki K. 2005. Snail accelerates cancer invasion by upregulating MMP expression and is associated with poor prognosis of hepatocellular carcinoma. Br J Cancer 92:252–258.

Nakai K, Kawato T, Morita T, Iinuma T, Kamio N, Zhao N, Maeno M. 2013. Angiotensin II induces the production of MMP-3 and MMP-13 through the MAPK signaling pathways via the AT(1) receptor in osteoblasts. Biochimie 95:922–933.

Nakamura T, Naruse M, Chiba Y, et al. 2015. Novel hedgehog agonists promote osteoblast differentiation in mesenchymal stem cells[J]. J Cell Physiol 230(4):922–929.

Saito W, Uchida K, Ueno M, Matsushita O, Inoue G, Nishi N, Ogura T, Hattori S, Fujimaki H, Tanaka K, Takaso M. 2014. Acceleration of bone formation during fracture healing by injectable collagen powder and human basic fibroblast growth factor containing a collagen-binding domain from Clostridium histolyticum collagenase. J Biomed Mater Res A 102:3049–3055.

Scholes S, Panesar S, Shelton NJ, Francis RM, Mirza S, Mindell JS, Donaldson LJ. 2014. Epidemiology of lifetime fracture prevalence in England: A population study of adults aged 55 years and over. Age Ageing 43:234–240.

Shenoy A, Blelloch RH. 2014. Regulation of microRNA function in somatic stem cell proliferation and differentiation. Nat Rev Mol Cell Biol 15:565–576.

Shiomi T, Lemaitre V, D'Armiento J, Okada Y. 2010. Matrix metalloproteinases, a disintegrin and metalloproteinases, and a disintegrin and metalloproteinases with thrombospondin motifs in non-neoplastic diseases. Pathol Int 60:477–496.

Siggeirsdottir K, Aspelund T, Jonsson BY, Mogensen B, Gudmundsson EF, Gudnason V, Sigurdsson G. 2014. Epidemiology of fractures in Iceland and secular trends in major osteoporotic fractures 1989–2008. Osteoporos Int 25:211–219.

Stewart CM, Kiner D, Nowotarski P. 2013. Intramedullary nail fixation of fibular fractures associated with tibial shaft and pilon fractures. J Orthop Trauma 27:e114–e117.

Trompeter HI, Dreesen J, Hermann E, Iwaniuk KM, Hafner M, Renwick N, Tuschl T, Wernet P. 2013. MicroRNAs miR-26a, miR-26b, and miR-29b accelerate osteogenic differentiation of unrestricted somatic stem cells from human cord blood. BMC Genomics 14:111.

Vimalraj S, Partridge NC, Selvamurugan N. 2014. A positive role of microRNA-15b on regulation of osteoblast differentiation. J Cell Physiol 229:1236–1244.

Wu Q, Jin H, Yang Z, Luo G, Lu Y, Li K, Ren G, Su T, Pan Y, Feng B, Xue Z, Wang X, Fan D. 2010. MiR-150 promotes gastric cancer proliferation by negatively regulating the pro-apoptotic gene EGR2. Biochem Biophys Res Commun 392:340–345.

Yokobori T, Suzuki S, Tanaka N, Inose T, Sohda M, Sano A, Sakai M, Nakajima M, Miyazaki T, Kato H, Kuwano H. 2013. MiR-150 is associated with poor prognosis in esophageal squamous cell carcinoma via targeting the EMT inducer ZEB1. Cancer Sci 104:48–54.

Yoon WJ, Cho YD, Kim WJ, Bae HS, Islam R, Woo KM, Baek JH, Bae SC, Ryoo HM. 2014. Prolyl isomerase Pin1-mediated conformational change and subnuclear focal accumulation of Runx2 are crucial for fibroblast growth factor 2 (FGF2)-induced osteoblast differentiation. J Biol Chem 289:8828–8838.

Zhang N, Wei X, Xu L. 2013. MiR-150 promotes the proliferation of lung cancer cells by targeting P53. FEBS Lett 587:2346–2351.